CHAPTER 241

Hydraulic Approach to Determining Optimum Interval of Discharge Sites of Barge in Constructing Rubble Foundation of Deep Water breakwater

Yoshiharu Matsumi [1] Akira Kimura [2]

Abstract

This study aims to establish the effective and economical construction scheme of the rubble mounds which are constructed by discharging a large amount of rubble from hopper barge. Since the plane scatter of the landing rubble on the sea floor directly depends on the random drift force exerted on the settling rubble, the statistical properties for the scattering range of the settling rubble in the still water are fully investigated in experiments. On the basic of the experiments and the discrete block method which equipped to cope with the steeper slope of rubble mound than the angle of repose for rubble, a numerical technique to simulate the spatial geometry of the discharged rubble on the sea floor taking the angle of repose for the rubble into account is developed. An optimum interval of the discharge sites of the barge which makes the uneven property of the mound's surface minimum is discussed in connection with the change in the the design water depth of breakwater and the discharge times.

1 Introduction

Caisson type breakwater is usually placed on a rubble mound foundation. In general the foundations are constructed by discharging a large amount of rubble from hopper barges. An adavntage of this construction method exists in its rapid "executability", since barges can carry a large volume of rubble at one time. However the mounds by individual discharge from the barge tend to form uneven surface, since the rubble landing on sea floor distributes widely. This is a drawback of this construction method. Since the design water depth of breakwaters has become deeper and the size of the rubble mound has become greater,

[1]Associate Prof. Dept. of Social Systems Engg., Faculty of Engg., Tottori Unversity. 4-101 Koyama-Minami, Tottori, 680, Japan.

[2]Professor, Dept. of Social Systems Engg., Faculty of Engg., Tottori Unversity.

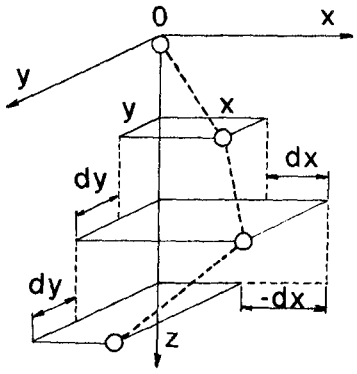

Figure 1: Definition of the fluctuation of the settling rubble.

the portion of the rubble foundation work to the total process of breakwater construction has been increasing. Therefore, the technique to construct a mound for breakwaters effectively and economically has become very important. This study aims to establish the effective construction scheme of the rubble mound by using a hopper barge, firstly the statistical properties of the landing rubble distributions on the sea floor are investigated with the experiments, secondly a numerical technique to simulate the spatial geometry of the discharged rubble mound from hopper barges by taking the angle of repose for the rubble into acount is developed. Finally, the effective interval of the discharge points of the barges which minimizes the uneven property of the mound's surface is discussed in connection with the spatial geometry of the rubble mound by multi-discharge and the water depth.

2 Stochastic properties for scattering position of settling rubble in still water

In the experiments, the representative sizes of rubble $d = 2.8\,cm$, $3.7\,cm$ and $4.3\,cm$ are employed. Experiments have been carried out in a laboratory settling tank with $2\,m$ depth and $1.1m \times 1.1m$ cross-section. Every piece of rubble is dropped from same position on the water surface. The total amount of settled rubbles is 3000 for each rubble diameter. At six different water depths, the x and y positions of the settling rubble are measured by two video cameras (Figure 1, x, y; horizontal axes, z; vertical axis). O is the discharge point of rubble, dx and dy are the displacements between specified depths in x and y direction. The stochastic properties for dx and dy at every water depth are investigated.

Figure 2 shows the distributions for dx and dy at six different water depths. These experiments are the case for the average diameter $d = 2.8\,cm$. The shapes of distributions are similar to each other except for the case of $z/d = 7.1$. The

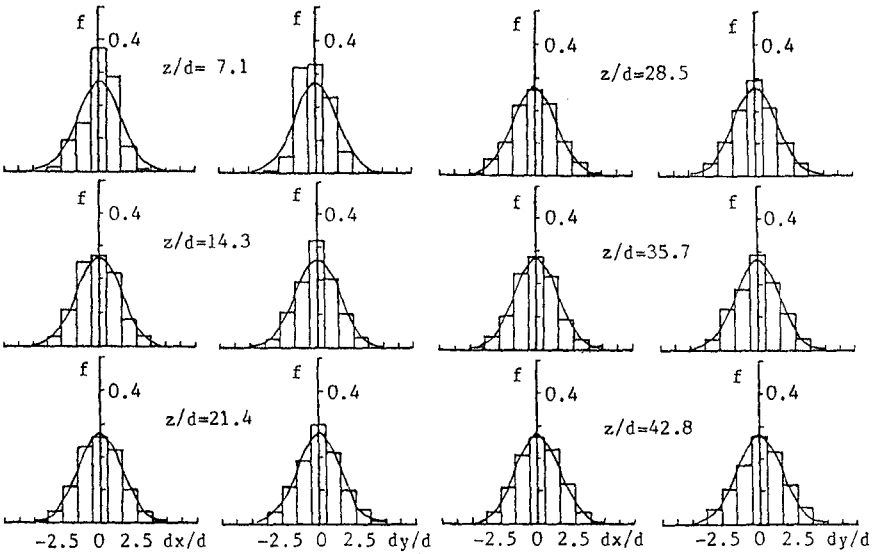

Figure 2: Distributions for dx/d and dy/d at six different water depth.

cases for other diameters are the same properties to this case. Therefore, it may be considered that the stochastic property for the displacement of the settling rubble at every section is identical.

Figure 3 shows the change in the mean values $(dx_m/d, dy_m/d)$ and the standard deviations (σ_X, σ_y) with respect to the relative water depth from the still water surface. Though the values of dx_m/d and dy_m/d at every section show a random fluctuation with changing z/d, the fluctuation range is less than about 10% of rubble diameter. On the other hand, no practical difference in standard deviations σ_x and σ_y at every section except for $z/d = 7.1$ is observed. From these investigations, the stochastic properties for the displacement of the settling rubble at every section may be assumed to be identical. In this study, the means for dx and dy at every section are assumed to be zero, σ_x and σ_y are assumed to be equal at every section.

3 Stochastic simulation technique for spatial geometry of rubble mound discharged from hopper barge

3.1 Probability distribution for settling position of rubble

In this study, the distribution for the displacement of the settling rubble at every section is assumed to be estimated by the Gaussian distribution with zero mean

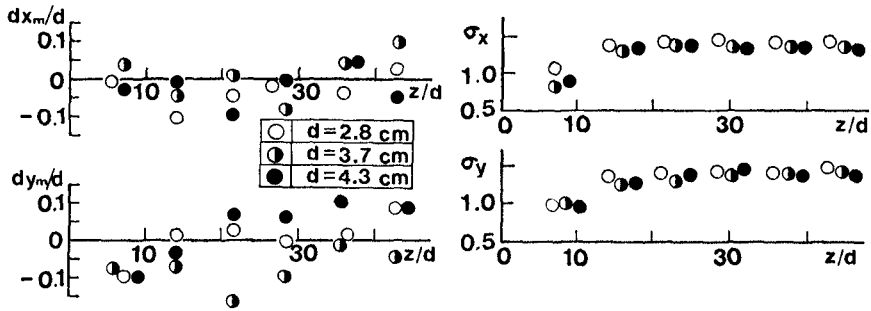

Figure 3: Change in the mean values and the standard deviations for dx/d and dy/d with changing water depth.

value as following:

$$f(x^*) = \frac{1}{\sqrt{2\pi}\,\sigma} \exp\left\{-\frac{1}{2}\left(\frac{x^*}{\sigma}\right)^2\right\} \tag{1}$$

$$f(y^*) = \frac{1}{\sqrt{2\pi}\,\sigma} \exp\left\{-\frac{1}{2}\left(\frac{y^*}{\sigma}\right)^2\right\} \tag{2}$$

where $\sigma = (\sigma_x + \sigma_y)/2$, $x^* = x/d$, $y^* = y/d$. In Figure 2, the solid lines are the calculations of Eq. (1), (2). The calculations and the experiments except for $z/d = 7.1$ agree reasonably well. The other cases for the rubble diameter were same results also. From these investigations, it may be considered that the stochastic properties for the displacement of the settling rubble at every section are identical and stationary process. Therefore, applying the Markov chain theory to the stochastic process for the displacement of the settling rubble, the stochastic model to estimate the distribution for the settling position of rubble is developed In this study.

The situation space vector S for the settling position of one piece of rubble in this stochastic model is defined as

$$S = \{-r, -r+1, \ldots, 0, \ldots, r-1, r\} \tag{3}$$

where $r(= x/d = y/d)$ is the relative longest distance of the plane scatter of the landing rubble on the sea floor in the x and y direction, and r is the positive integral constant. Then, the transition probability matrix P is given by

$$P = [\ p(i,j)\ ] \qquad i = -r \sim r,\ j = -r \sim r \tag{4}$$

where

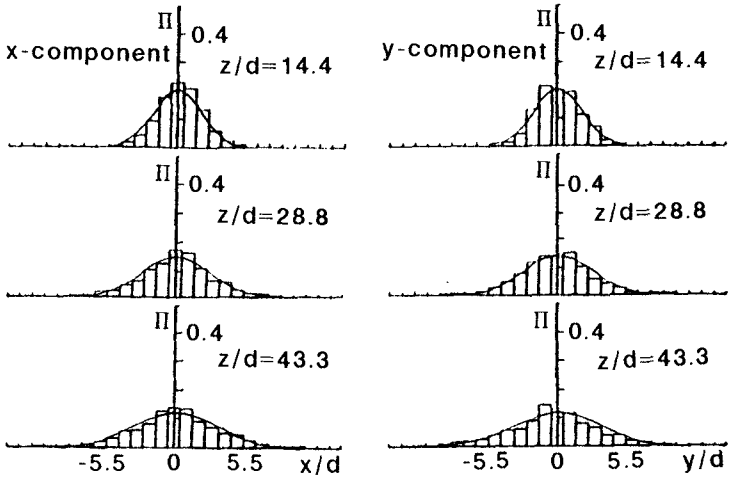

Figure 4: Probability distribution for the settling position of rubble at different water depth.

$$\begin{array}{ll} i-j=0 & p(i,j)=p_0 \\ i-j=-k & p(i,j)=p_k^+ \\ i-j=k & p(i,j)=p_k^- \\ |i-j|>k & p(i,j)=0 \\ & (k=1,2,\ldots,6) \end{array}$$

in which $p(i,j)$ is a transition probability that the rubble settles from the i-th position at the m-th section to the j-th position at the $m+1$-th section, p_0 and p_k are the probabilities for the cases in which the displacement of the settling rubble at a section is 0 and k respectively, these values can be calculated from Eq. (1) and (2). Then the probability distribution for the settling position of rubble is given by

$$\begin{aligned} \Pi(m) &= \Pi(m-1)\cdot P \\ \Pi(0) &= [\underbrace{0,\ldots,0}_{r},1,\underbrace{0,\ldots,0}_{r}] \end{aligned} \tag{5}$$

where $\Pi(0)$ is the probability vector for the initial position of rubble at dropping. Figure 4 shows examples of the experimental distributions and the calculated results for the setlling position of rubble (solid line). The present stochastic model can simulate the shape of distributions regardless of the relative water depth with sufficient accuracy.

Table 1 shows the correlation coefficient of dx/d and dy/d at every sections. The values of correlation coefficient except for $z/d = 7.1$ may be approximately zero

Table 1: Correlation coefficient between dx/d and dy/d.

Section	$d = 2.8\ cm$	$d = 3.7\ cm$	$d = 4.3\ cm$
$z/d = 7.1$	0.176	0.129	0.136
$z/d = 14.3$	0.019	0.006	−0.012
$z/d = 21.4$	−0.002	0.013	−0.021
$z/d = 28.5$	0.017	0.003	−0.047
$z/d = 35.7$	−0.008	0.025	−0.044
$z/d = 42.8$	0.032	0.023	−0.058

regardless of the sections and the case. Therefore, it may be considered that the stochastic properties for the displacements of the settling rubble in the x and y direction are indepentent. Then the probability distribution of the plane scatter for the settling position of rubble is given by

$$p_r(x^*, y^*) = \Pi_x \cdot \Pi_y \tag{6}$$

where Π_x and Π_y can be calculated from Eq. (6).

3.2 Spatial geometry of rubble mound discharged from hopper barge

The spatial geometry of individual rubble mound discharged from a hopper barge can be evaluated by combining the volume of rubble at discharge with a probability distribution of the plane scatter for the landing rubble on the sea floor. This probability distribution of can be evaluated as

$$P_r(j) = \left\{ \sum_{i=1}^{N} p_{ri}(j) \right\} / N \tag{7}$$

where N is the number of the panels which divid the hopper mouth into the $d \times d$ plane size in the numerical calculations (Matsumi Y.;1990), $p_{ri}(j)$ is a probability that the rubble which is fallen from the i-th discrete portion in the hopper mouth lands to the j-th discrete portion on the sea floor. The probability $p_{ri}(j)$ can be calculated from the probability distribution for the settling position of rubble (Eq. (6)). Finally, the spatial geometry of rubble mound which is discharged from a barge can be simulated by

$$H(j) = V \cdot P_r(j)/d^2 \tag{8}$$

where $H(j)$ is the mound height in the j-th discrete portion on the sea floor, V is the volume of rubble at discharge.

Figure 5 shows the comparison of heights of the calculated rubble mounds by the present stochastic simulation technique and experimental data by Okude et al.

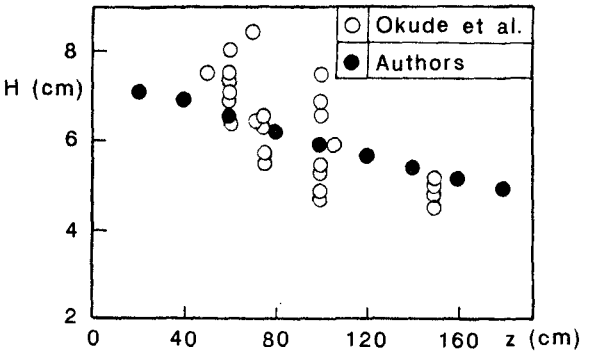

Figure 5: Comparison bwteen height of calculated rubble mounds and experiments.

(1982), in case for the rubble mound which is formed by an single discharge. In the experiments of Okude et al., a 1/20 scale model hopper barge with 100 m^3 hopper volume was employed. It may be concluded that the spatial geometry of rubble mounds formed by an single discharge can be evaluated with sufficient accuracy by the present stochastic simulation technique.

4 Simulation technique for rubble mound at multi-discharge

In the case for rubble mound formed by multi-times discharge from the same position, the slope of rubble mound approaches the angle of repose for the rubble with increasing discharge times. Then, the rolling rubbles and the sliding those on the slope may occur. The present stochastic simulation technique cannot cope with those phenomena which are recognized in the experiments. Therefore, to cope with the steeper slope of rubble mound than the angle of repose for rubble, the correctional model for the stochastic technique is investigated through the experiments and the numerical calculations.

Experiments have been carried out in a laboratory settling tank with $1.5m$ depth and $2m \times 2m$ cross-section. The hopper barge model used was a 1/20 scale model with 100 m^3 hopper volume. The representative sizes of rubble d = 2.8 cm, 3.7 cm and 4.3 cm are employed in the experiments. The height and width of the rubble mound formed by multi-times discharge from the same position were measured by two video cameras which were allocated in the directions of barge width and length. Furthermore, the change in the shape of cross section of the discharged mound with respect to the discharge time was investigated. From the experiments, it has been found that the shape of cross section of the rubble mound formed by multi-times discharge can be classified into three patterns, namely, as the discharge time increases, the sectional shape of rubble mound

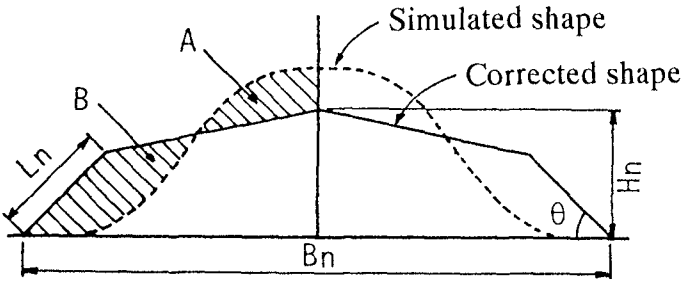

Figure 6: Correctional model for cross section of simulated rubble mound.

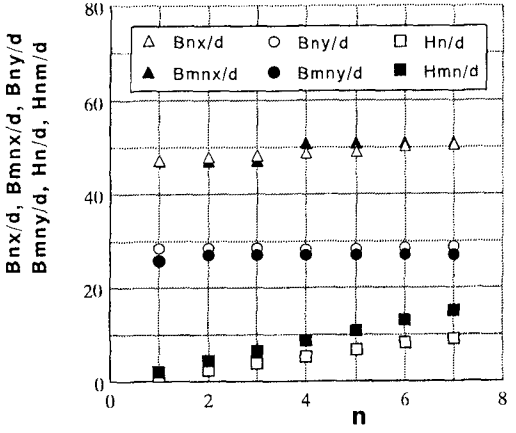

Figure 7: Comparison of calculations for width and height of mound with experiments

transforms from a trapezoidal shape into a pentagonal shape and further into a triangular shape with slope of the angle of repose for the rubble.

From these shape properties of cross section of the rubble mound, a correctional model for the shape of cross section of the simulated mound by the present stochastic technique is devised as shown in Figure 6. In this figure, the dotted line is the cross section of the simulated mound, the solid line is the corrected shape, H_n and B_n are the height and width of the corrected mound respectively, θ is the angle of repose for rubble. In the case for $H_n \geq L_n \cdot \sin\theta$, the shape of cross section of the simulated mound is corrected to the trapezoidal shape or the pentagonal shape such that the areas of shadowed portions A and B become equal. On the other hand, in the case for $H_n \leq L_n \cdot \sin\theta$, the shape of cross section of the simulated mound is corrected to the triangular shape with the angle of repose for rubble.

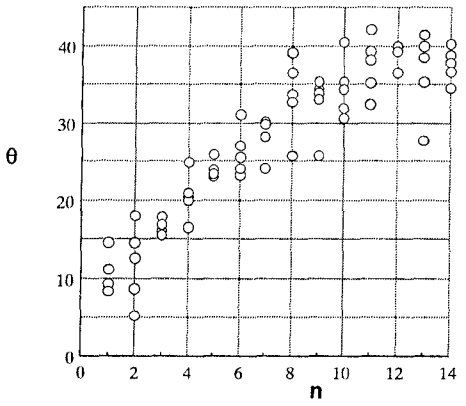

Figure 8: Change in measured θ with respect to n.

The values of H_n and B_n in Figure 6 have been given by comparing the calculations for the height and width of the mound at every time discharge with the experiments as shown in Figure 7, in which the abscissa n is the number of discharge time. B_{nx} and B_{ny} are the measured width in the barge length and width directions respectively, B_{mnx} and B_{mny} are the calculated those, H_n and H_{mn} are the measured height and the calculated that. This Figure is the case for the water depth $h = 60\,cm$. It is found that the calculations for the width of the mound at every time discharge agree with the experiments reasonably well. However, since the present stochastic simulation technique cannot cope with the sliding rubbles and the rolling those on the slope of mound, the calculations for the height and the experiments markedly become to disagree with increasing the discharge time. Then, from the investigation on the relationship between the simulated heights of the mound at every discharge and the measurements, it has been found that a linear relationship between H_{mn} and H_n is established and H_n is given by

$$H_n = 0.6 H_{mn} \tag{9}$$

Figure 8 shows the change in the angle of slope of the measured mound with respect to the number of discharge time n. The values of θ show a tendency to approache to about 40° with increasing n. However, since the measured data vary widely, when reading a value of the angle of repose for the rubble from these results, the error of reading becomes very large. Then, the discrete block method (Cundall P.A.,1971, 1976) are applyed to analyze the angle of repose for rubble numerically.

In the discrete block method, the rubble is approximately replaced by a circular element as shown in Figure 9. The elastic and inelastic characteristics of rubble are modeled by an elastic spring (spring coefficient; K), a viscous dashpot (vis-

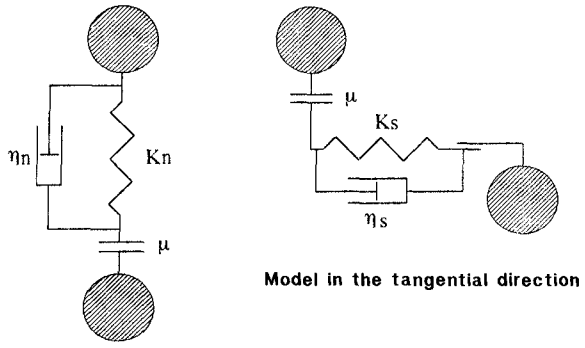

Figure 9: Dynamic system in the discrete block method.

cous coefficient; η) and a frictional slider (friction coefficient; μ). The behaviours of the rolling and sliding rubbles on the slope of mound can be numerically simulated by solving the simultaneous common differential eqautions which are set up for the translational and rotational motions for every rubble element. The equations of the translational and rotational motion for every rubble element are given as following difference equations including unknown variables u, v and ϕ explicitly.

$$\begin{aligned}
&(m + C_M \rho_W V_S)[\ddot{u}]_t = \\
&\quad -\eta[\dot{u}]_{t-\Delta t} - K[u]_{t-\Delta t} - 0.5\rho_W C_D d|[\dot{u}]_{t-\Delta t}|[\dot{u}]_{t-\Delta t} \\
&\quad +(\rho_S - \rho_W) V g \\
&(m + C_M \rho_W V_S)[\ddot{v}]_t = \\
&\quad -\eta[\dot{v}]_{t-\Delta t} - K[v]_{t-\Delta t} - 0.5\rho_W C_D d|[\dot{v}]_{t-\Delta t}|[\dot{v}]_{t-\Delta t} \\
&I[\ddot{\phi}]_t = -(\eta[\dot{\phi}]_{t-\Delta t} + K[\phi]_{t-\Delta t})\, d^2/4
\end{aligned} \tag{10}$$

where u and v are the displacements of rubble element in the vertical and horizontal motions, ϕ is the angle of element in the rotational motion, m and V_S are the mass and volume of it, I is the inertia moment of it, ρ_S and ρ_W are the density of rubble and fluid, C_D and C_M are the drag coefficient ($=1.0$) and the added-mass coefficient ($=2.0$) of rubble and Δt is the time interval of numerical calculation. Since the rubble is modeled by a circular element in this study, to prevent the modeled rubble after landing on the sea floor from the rolling motion in the horizontal direction, the sea floor is replaced by the ripples with the diameter of rubble element. In the numerical calculations, the spring coefficients (K_n, K_s), the viscous coefficients (η_n, η_s) and the frictional slider coefficient (μ) adopt values listed in Table 2 which contains both cases for the rubble to rubble and the rubble to sea floor respectively. The difference between the values of

Table 2: Values of K, η, μ and Δt.

Coefficient	Rubble to rubble	Rubble to sea floor
$K_n/\rho_s g\ (cm)$	3.64×10^4	$(1/5)3.64 \times 10^4$
$K_s/\rho_s g\ (cm)$	9.48×10^3	$(1/5)9.48 \times 10^3$
$\eta_n/\rho_s g\ (cm/s)$	2.18×10	$(1/5)2.18 \times 10$
$\eta_n/\rho_s g\ (cm/s)$	2.18×10	$(1/5)2.18 \times 10$
μ	$\tan 30°$	$\tan 10°$

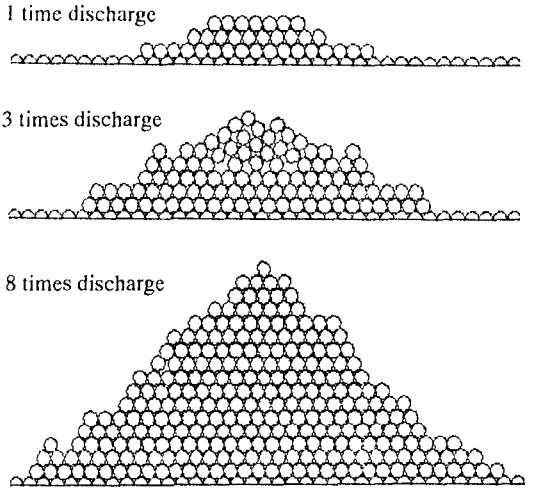

Figure 10: Simulated cross section of rubble mound formed by 1, 3 and 8 times discharge.

coefficients in the case for rubble to rubble and those for rubble to sea floor is to deal successfully with a buffer action effect due to the sand bed in the sea floor. The time interval of the numerical calculation Δt is 1.0×10^{-4}s. The initial positions of rubble elements in the numerical calculations are densely arranged in the simulated cross section by the present stochastic simulation technique. The initial settling velocity of every element in the vertical direction adopts the sinking velocity of rubble ($60\ cm/s$) which has been clarified from the experiments. The calculations in the case for the multi-times discharge were carried out by such method that the rubble elements at the following discharge are fallen on the simulated mound at the previous discharge.

Figure 10 shows the simulated cross section of rubble mound formed by one, three and eight times discharge from the same discharge point. As the number of discharge time increses, the shape of the cross section of rubble mound trans-

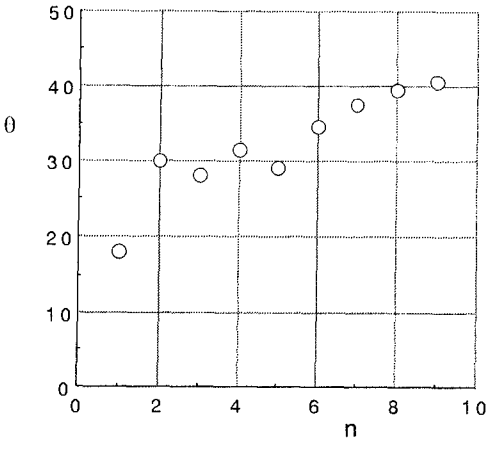

Figure 11: Change in calculated θ with respect to n.

forms from the trapezoidal shape into the pentagonal shape and further into the triangular shape. Therefore, it can be concluded that the present technique simulates the dominant features which are recognized in the experiments with reasonable well. The angles of the slope of mound at every discharge which are read from the cross section of the rubble mound calculated through the discrete block method are shown in Figure 11. It is found that θ approaches to about 40° with increasing n. Therefore, the angle of repose for the rubble is estimated to be 40° in this study, this value is adopted in the present correctional model.

To investigate the application of the present correctional technique, the width and height of the corrected cross section of rubble mound are copmared with the experiments in the case for $h = 120\,cm$ as shown in Figure 12, in which the white and black symbols indicate the experiments and the calculations respectively. Firstly, though the calculated width B_{nxc}/d of the mound in the barge length direction can evaluate the change in the experiments B_{nx}/d with respect to n, the calculations overestimate the experiments. Secondly, in the case for the mound width in the barge width direction, B_{ny}/d and B_{nyc}/d agree with sufficient accuracy. Finally, the calculations H_{nc}/d for the height of the mound agree well with the experiments H_n/d. Therefore, it may be concluded that the shape of the cross section of rubble mound formed by multi-times discharge from the same point can be evaluated by combining the stocahstic simulation technique with the present correctional technique. However, the applicable limitation of this correctional technique for the case of the barge length direction is not sufficiently made clear in this study.

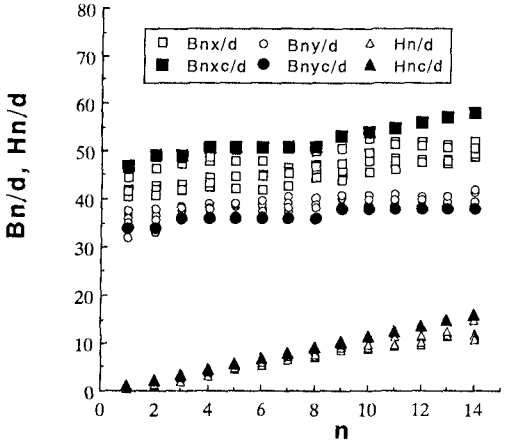

Figure 12: Comparison of calculations for width and height of mound with experiments.

5 Optimal Interval of Discharge Sites of Barge

In this study, the optimal interval of discharge sites of barge is defined as a distance between discharge points from barges which minimizes the uneven property of the mound's surface. Figure 13 shows the change in the size of the gap between mounds with respect to the relative interval of the discharge sites of the barge, in which δ is the gap size between individual mounds, H is the representative height of mound and a is the distance between the discharge sites of barges. These calculations are the case for 2, 6 and 10 times discharge at two kinds of relative water depths $h/d = 42.8$ and 71.4. The effective interval of the discharge sites of the barge can be determeined by this figure. Comparing the case for $h/d = 42.8$ with $h/d = 71.4$, when the water depth is deeper, the interval of the discharge points of the barge which makes the uneven property of the mound's surface minimum becomes longer. Therefore, it may be concluded that when deciding the interval of the discharge sites of the barge, the design water depth of breakwater becomes the important parameter.

6 Conclusion

Concluding remarks are as follows:
(1) The stochastic properties for the displacement of the settling rubble at every section are identical and the stationary process. The stochastic simulation techinque which is developed by applying the Markov chain model can estimate the distribution for the settling posiotion of rubble regardless of the relative water with sufficient accuracy.

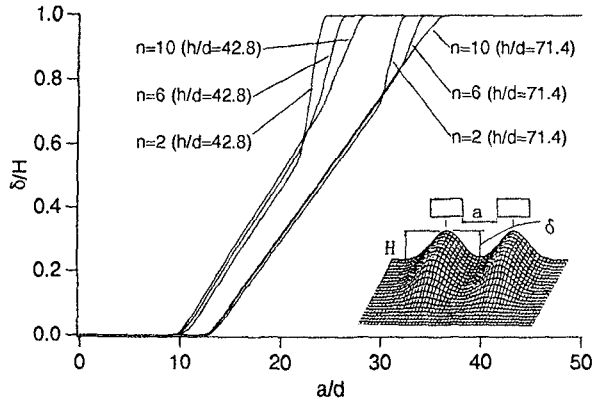

Figure 13: Change in the gap size between mounds with respect to the relative interval of discharge point of barges.

(2) The angle of repose for the rubble can be numerically calculated by applying the discrete block method. The spatial geometry of the multi-times discharged rubble mound from the same point can be successfully simulated by combining the present stochastic technique with the present correctional technique. However, applying this combined simulation technique for the case of the barge length direction, the problem of how to deal with the width of the mound remains still.
(3) The effective interval of the discharge points from barges which makes the uneven property of the mound's surface minimum in the case for the barge width direction is clarifyed in connection with the design water depth of breakwater and the number of discharge times.

References

Cundall P.A.(1971): A computer model for simulating progressive, Large scale movements in blocky rock systems, Symp. ISRM, Nancy, France, Proc. Vol.2, pp.129-136.

Cundall P.A.(1976): Explicit finite-difference method in geomechanics, Numerical methods in geomechanics (edited by Desai C.S.), Vol.1, pp.132-150.

Matsumi Y.(1990): A fundamental study on construction scheme for rubble foundation of deep water breakwater from hopper barge, 22nd Inter. Conf. on Coastal Engg.(ASCE), pp.1648-1661.

Okude T., et al.(1982): Experimental study on construction of rubble mound by split hopper barge, Report of the Port and Harbour Research Institute, Vol.21, No.4, pp.132-171. (in Japanese)